



Title	Statistical interactions of multiple oxide traps under BTI stress of nanoscale MOSFETs
Author(s)	Markov, Stanislav; Amoroso, Salvatore Maria; Gerrer, Louis; Adamu-Lema, Fikru; Asenov, Asen
Citation	IEEE Electron Device Letters, 2013, v. 34, n. 5, p. 686-688
Issued Date	2013
URL	http://hdl.handle.net/10722/221391
Rights	IEEE Electron Device Letters. Copyright © IEEE

Statistical Interactions of Multiple Oxide Traps Under BTI Stress of Nanoscale MOSFETs

Stanislav Markov, *Member, IEEE*, Salvatore Maria Amoroso, *Member, IEEE*, Louis Gerrer, Fikru Adamu-Lema, *Member, IEEE*, and Asen Asenov, *Fellow, IEEE*

Abstract—We report a thorough 3-D simulation study of the correlation between multiple, trapped charges in the gate oxide of nanoscale bulk MOSFETs under bias and temperature instability (BTI). The role of complex electrostatic interactions between the trapped charges in the presence of random dopant fluctuations is evaluated, and their impact on the distribution of the threshold voltage shift and on the distribution of the number of trapped charges is analyzed. The results justify the assumptions of a Poisson distribution of the BTI-induced trapped charges and of the lack of correlation between them, when accounting for time-dependent variability in circuits.

Index Terms—Bias and temperature instability (BTI), complimentary metal–oxide–semiconductor (CMOS), random telegraph noise (RTN), reliability, variability.

I. INTRODUCTION

ONE of the biggest challenges that complimentary metal–oxide–semiconductor (CMOS) reliability-aware design methodology faces today is the statistical variability in nanoscale transistors, due to the discreteness of charge and granularity of matter [1], [2]. The interplay between statistical variability and the degradation phenomena in transistors implies that their performance- and reliability-related parameters must be evaluated as stochastic variables [3]–[5]. It is now experimentally established that the capture and emission dynamics of oxide traps underlie both random telegraph noise (RTN) and bias-temperature instability (BTI) [6], thus motivating the inclusion of these effects in statistical simulations of contemporary devices and circuits [2], [7]–[9]. However, all previous statistical simulation studies assume that trapped charges act as uncorrelated sources of noise, and that the number of trapped charges remains Poissonian at all times. Although the statistics of trapped charges have been

experimentally addressed [9], these two assumptions remain questionable for ultrascaled CMOS, as their validity at least in the context of Flash-memory cells is limited [11]–[13].

We examine the aforementioned assumptions via 3-D device simulations of the statistical effects related to multiple trapped charges in the gate oxide of decananometer MOSFETs, taking into account the complex 3-D electrostatic effects and the stochastic charge injection determining the degradation of the threshold voltage V_T over time.

II. SIMULATION METHODOLOGY

This letter is based on the 3-D “atomistic” drift-diffusion simulator GARAND, with density-gradient quantum corrections [14]. Coupling the simulator to a kinetic Monte Carlo (KMC) engine enables time-domain simulations in the presence of oxide traps, by modeling the dynamics of each trap and its interactions with neighboring traps, in conjunction with the sources of variability [16]. The average injection time $\bar{\tau}_{inj} = q \exp(E_a/k_B T) / \int_{\sigma} J_{WKB}(x, y) dx dy$, (q —unit charge, $\sigma = 10^{-14}$ cm² trap cross section, J_{WKB} —1-D direct tunneling current to the trap, E_a —activation energy in the multiphonon-correction factor) governs the trapping kinetics [13], [16], trap creation/anneal, and emission not being considered here. The traps are located 3.3 eV below the oxide conduction band. The test device is a square, n-channel, bulk MOSFET with a 25 nm physical gate length, 1.2 nm SiO₂ gate oxide, and halo implants [15].

III. CORRELATION EFFECTS IN ΔV_T DISTRIBUTION

To evaluate how the interactions between N multiple charges affect the distribution of the threshold voltage shift, $\Delta V_{T,N}$, we simulate ensembles of 2000 devices with RDF, each device having the same number of trapped electrons, N . The electron charges are uniformly distributed throughout the volume of the oxide. Fig. 1 shows the mean and variance of $\Delta V_{T,N}$ normalized to the mean and variance of the one-electron-induced shift $\Delta V_{T,1}$ versus the number of trapped charges N . The linear relation with a slope of 1 suggests that each trap contributes independently to $\Delta V_{T,N}$, even for very heavy BTI (30 traps $> 5 \times 10^{12}$ cm⁻²). Fig. 1 also reports the exact values of the mean μ and standard deviation σ of $\Delta V_{T,N}$. They remain constant when normalized by N , as expected from uncorrelated traps. In lack of correlation, one can imply the distribution of $\Delta V_{T,N}$ by self-convolving $N-1$ times the distribution of $\Delta V_{T,1}$. This is proven in Fig. 2, by

Manuscript received February 18, 2013; revised March 10, 2013; accepted March 16, 2013. Date of current version April 22, 2013. This work was supported in part by the European Project MORDRED (EU Project 261868) and the Area of Excellence on Nanoelectronics of the University Grant Council of Hong Kong under Project AoE/P-04/08. The review of this letter was arranged by Editor J. Schmitz.

S. Markov was with the Device Modeling Group, University of Glasgow, Glasgow G12 8LT, U.K. He is now with the Department of Chemistry, The University of Hong Kong, Hong Kong (e-mail: figaro@hku.hk).

S. M. Amoroso, L. Gerrer, and F. Adamu-Lema are with the Device Modeling Group, University of Glasgow, Glasgow G12 8LT, U.K. (e-mail: salvatore.amoroso@glasgow.ac.uk).

A. Asenov is with the Device Modeling Group, University of Glasgow, Glasgow G12 8LT, U.K., and also with Gold Standard Simulation, Ltd., Oakfield Avenue, Glasgow G12 8LT, U.K.

Color versions of one or more of the figures in this letter are available online at <http://ieeexplore.ieee.org>.

Digital Object Identifier 10.1109/LED.2013.2253541

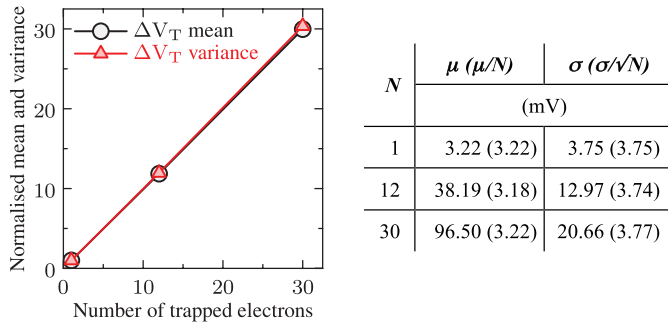


Fig. 1. Mean μ and variance σ^2 of the multielectron-induced $\Delta V_{T,N}$ normalized by the corresponding one-electron-induced $\Delta V_{T,1}$ values equal the number of trapped electrons (fixed across the device ensemble), as expected from independently acting fixed charges. However, normalization by N , tabulated to the right, reveals a hyperexponential character, since $\mu/N > \sigma/N$.

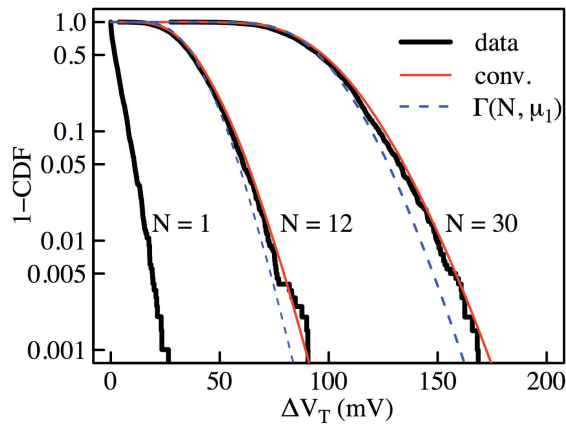


Fig. 2. Comparison between the cumulative distributions of $\Delta V_{T,N}$ and the corresponding convolutions of $\Delta V_{T,1}$. Convolution and data practically overlap and the influence of each trap can be considered independently. Gamma fit with an average μ_1 equal to $\Delta V_{T,1}$ is shown to underestimate the tail of the distribution.

comparing the result of such a convolution with the simulation data for the 12- and 30-trap-induced $V_{T,N}$. Therefore, although the ΔV_T contributed by a trap depends on the occupancy of the other traps [17], the overall distribution due to multiple traps can be described as $N-1$ self-convolutions of $\Delta V_{T,1}$.

The lack of correlation between multiple trapped charges justifies simpler models accounting for BTI degradation of transistors in circuit simulations [7]–[9], where the change in V_T due to the trapping of an extra charge is modeled by the addition of $\Delta V_{T,1}$, randomly selected from an exponential distribution. However, the values reported in Fig. 1 reveal that ΔV_T differs from an exponential (or gamma Γ , for $N > 1$) distribution, since $\sigma/\sqrt{N} > \mu/N$, despite the fixed number of traps across the device ensemble. A convolution approach assuming an exponential with $\mu = \mu(\Delta V_{T,1})$ underestimates the tail of $V_{T,N}$ —see $\Gamma(N, \mu_1)$ in Fig. 2. Assuming an exponential with $\mu = \sigma(\Delta V_{T,1})$ instead, one can perfectly fit the slope of $\Delta V_{T,N}$ at the cost of enlarging the average $\Delta V_{T,N}$ (not shown for clarity). Therefore, if μ_1 and σ_1 are known from experiment or physical level device modeling, one can apply statistical techniques to generate a hyperexponential

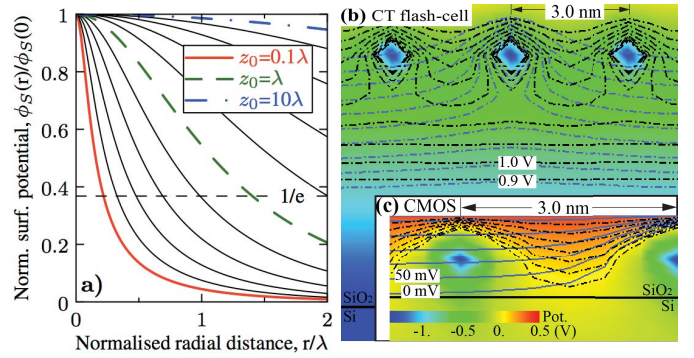


Fig. 3. (a) Attenuation of the surface-potential perturbation with radial distance r , for different trap-to-surface distance z_0 , based on the model of [18]. Normalization to bulk-screening length λ makes the plot independent of λ . (b) and (c) 2-D potential across the middle of the oxide of a CT Flash cell/MOSFET, with 20/1.2 nm oxide and fixed charges at 6.5/0.6 nm above the Si-oxide interface, at the same subthreshold drain current and an intertrap distance of 3 nm. Black potential contours are spaced at 100/50 mV. Blue contours are the same equipotentials, obtained from a simulation with only one trapped electron. The contours barely interact in (c), $z_0 < \lambda$, but strongly in (b), $z_0 > \lambda$.

random variate for the single-trap-induced ΔV_T in circuit simulations. The inequality $\sigma/\sqrt{N} > \mu/N$ likely stems from the following. Trapped charges above the channel interact strongly with the RDF underneath and determine the tail of the dispersion, while trapped charges above the source/drain overlap regions incur a smaller shift and effectively lower the average.

We note that correlation between multiple trapped electrons has been reported for charge-trapping (CT) nonvolatile memory cells [11]. In this case, the trapped charges are at a distance from the Si interface z_0 that is of the order of or larger than the bulk screening length λ of about 5–6 nm. On the contrary, in a CMOS transistor with thin gate oxide (~ 1 nm), the trapped charges are at $z_0 < \lambda$. In the latter case, the potential perturbation decays much faster, as theoretically shown in [18] and illustrated in Fig. 3(a), and suggests a weaker interaction between traps than in the former case, and hence lack of correlation effects. Fig. 3(b) and (c) shows potential contours in the oxide obtained from 3-D simulation of our 25 nm MOSFET and a flash cell as in [11], with an intertrap distance of 3 nm (density slightly over 10^{13} cm $^{-2}$). The contours in the middle between trapped charges are weakly affected for the thin dielectric ($z_0/\lambda < 1$), but strongly perturbed in the case of thick dielectric (large z_0/λ).

IV. CHARGE INJECTION STATISTICS

Here we analyze the distribution of the number of trapped charges N during BTI stress. At a fixed gate bias, the trapping of an electron in the oxide provides a negative feedback to the subsequent injection from the channel by lowering the oxide field, and reducing the inversion charge density. The corresponding increase in the capture-time constants of each trap leads to a sub-Poisson process with smaller variance than the average, $\sigma^2 N < \bar{N}$ [12]. For CT Flash cells, this phenomenon is revealed only after a relatively high number of electrons are trapped in the nitride layer [12], [13].

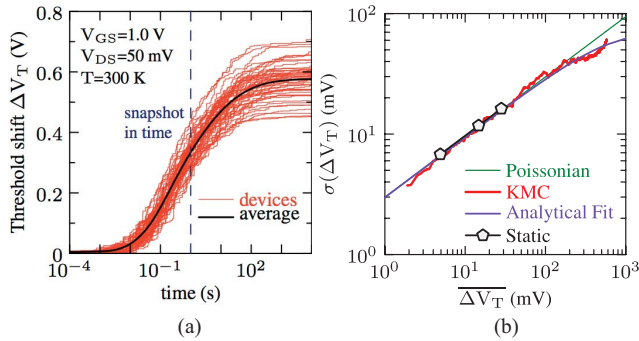


Fig. 4. (a) Evolution of ΔV_T with operational-BTI stress time for 50 MOSFETs with RDF and Poisson-distributed traps, initially empty. Vertical line represents the sampling of ΔV_T , and hence the number of trapped charges, at a given time. (b) Standard deviation versus average ΔV_T for “static” simulations, with Poisson-distributed trapped charges, and dynamic “KMC” simulations, from sampling the time evolution of ΔV_T in time. A Poissonian trend and an analytical fit as per [13], (1) are also shown.

However, for CMOS devices under BTI stress, the question remains open.

To answer it, we perform KMC-driven time-domain device simulations [16], and trace the evolution of ΔV_T with time, as a result of individual charge trapping events under BTI stress. An example of such simulation is reported in Fig. 4(a), illustrating the extraction of ΔV_T distribution at a given stress time. The dispersion of ΔV_T reflects the dispersion of the number of filled traps N , and is due not only to the interplay of RDF and random traps, but is strongly affected by the stochastic electron-injection process as well. Note that ΔV_T is directly observable (unlike N), and its statistics (i.e., mean and variance) obey the same trends as that of N [10], [12].

Fig. 4(b) shows the dependence of the standard deviation versus the average of ΔV_T , obtained from the time-domain simulations of 50 transistors (labeled KMC). A sign of sub-Poissonian behavior (dashed line) can be observed once $\overline{\Delta V_T} > 200$ mV. The onset of saturation is supported also by an analytical fit, as shown, based on (1) from [13] with a feedback parameter of 2. The large ΔV_T at which deviation from Poisson statistics becomes significant is reached at a trap density exceeding the levels of BTI-induced degradation. The symbols in Fig. 4(b) represent the “static” approach [3], where σV_T is evaluated from the static simulation of ensembles with different numbers of Poisson-distributed traps, up to a density of $\sim 3 \times 10^{12}$ cm $^{-2}$. At these trap densities, the static and dynamic simulations yield the same ΔV_T distributions.

V. CONCLUSION

We investigated two statistical aspects of the multitrapped-induced ΔV_T in nanoscale bulk MOSFETs—the electrostatic correlation between traps, and the distribution of their number over time. For trap densities associated with BTI degradation (up to 5×10^{12} cm $^{-2}$ [3]–[5]): 1) trapped charges act as uncorrelated sources of V_T fluctuations, and 2) the number of trapped charges during operational or BTI stress is well approximated by a Poisson distribution. At much higher trap density these assumptions may be violated, but breakdown phenomena would dominate the device characteristics in such a case. These results are fundamental for the development of

practical models and techniques that account for the time-dependent statistical variability in devices and circuits.

REFERENCES

- [1] S. Ghosh and K. Roy, “Parameter variation tolerance and error resiliency: New design paradigm for the nanoscale era,” *Proc. IEEE*, vol. 98, no. 10, pp. 1718–1751, Oct. 2010.
- [2] M. Nafria, R. Rodriguez, M. Porti, J. Martin-Martinez, M. Lanza, and X. Aymerich, “Time-dependent variability of high-k based MOS devices: Nanoscale characterization and inclusion in circuit simulators,” in *Proc. IEEE Int. Electron Devices Meeting*, Dec. 2011, pp. 127–130.
- [3] B. Cheng, A. R. Brown, and A. Asenov, “Impact of NBTI/PBTI on SRAM stability degradation,” *IEEE Electron Device Lett.*, vol. 32, no. 6, pp. 740–742, Jun. 2011.
- [4] G. D. Panagopoulos and K. Roy, “A three-dimensional physical model for V_{th} variations considering the combined effect of NBTI and RDF,” *IEEE Trans. Electron Devices*, vol. 58, no. 8, pp. 2337–2346, Aug. 2011.
- [5] M. Toledano-Luque, B. Kaczer, J. Franco, P. J. Roussel, T. Grasser, T. Y. Hoffmann, and G. Groeseneken, “From mean values to distributions of BTI lifetime of deeply scaled FETs through atomistic understanding of the degradation,” in *Proc. Symp. VLSI Technol.*, Jun. 2011, pp. 152–153.
- [6] T. Grasser, H. Reisinger, W. Goes, T. Aichinger, P. Hehenberger, P.-J. Wagner, M. Nelhiebel, J. Franco, and B. Kaczer, “Switching oxide traps as the missing link between NBTI and RTN,” *IEEE Trans. Electron Devices*, vol. 58, no. 11, pp. 3652–3666, Nov. 2011.
- [7] J. Fang and S. Sapatnekar, “Understanding the impact of transistor-level BTI variability,” in *Proc. IEEE Int. Rel. Phys. Symp.*, Apr. 2012, pp. CR.2.1–CR.2.6.
- [8] B. Kaczer, J. Franco, M. Toledano-Luque, P. J. Roussel, M. F. Bukhori, A. Asenov, B. Schwarz, M. Bina, T. Grasser, and G. Groeseneken, “The relevance of deeply scaled FET threshold voltage shifts for operation lifetimes,” in *Proc. IEEE Int. Rel. Phys. Symp.*, Apr. 2012, pp. 5A.2.1–5A.2.6.
- [9] K. Takeuchi, T. Nagumo, S. Yokogawa, K. Imai, and Y. Hayashi, “Single-charge-based modelling of transistor characteristics fluctuations based on statistical measurement of RTN amplitude,” in *Proc. Symp. VLSI Technol.*, Jun. 2009, pp. 54–55.
- [10] B. Kaczer, P. J. Roussel, T. Grasser, and G. Groeseneken, “Statistics of multiple trapped charges in the gate oxide of deeply scaled MOSFETs—Application to NBTI,” *IEEE Electron Device Lett.*, vol. 31, no. 5, pp. 411–413, May 2010.
- [11] A. Mauri, C. Compagnoni, S. M. Amoroso, A. Maconi, A. Ghetti, A. S. Spinelli, and A. L. Lacaita, “Comprehensive investigation of statistical effects in nitride memories—part I: Physics-based modeling,” *IEEE Trans. Electron Devices*, vol. 57, no. 9, pp. 2116–2123, Sep. 2010.
- [12] C. Compagnoni, R. Gusmeroli, A. Spinelli, A. Visconti, “Analytical model for the electron-injection statistics during programming of nanoscale Flash memories,” *IEEE Trans. Electron Devices*, vol. 55, no. 11, pp. 3192–3199, Nov. 2008.
- [13] A. Maconi, S. Amoroso, C. Compagnoni, A. Mauri, A. S. Spinelli, and A. L. Lacaita, “Three-dimensional simulation of CT memory programming—part II: Variability,” *IEEE Trans. Electron Devices*, vol. 58, no. 7, pp. 1872–1878, Jul. 2011.
- [14] [Online]. Available: <http://www.goldstandardsimulations.com>
- [15] F. Adamu-Lema, C. Compagnoni, S. Amoroso, N. Castellani, L. Gerrer, S. Markov, A. S. Spinelli, A. L. Lacaita, and A. Asenov, “Accuracy and issues of the spectroscopic analysis of RTN traps in nanoscale MOSFETs,” *IEEE Trans. Electron Devices*, vol. 60, no. 2, pp. 833–839, Feb. 2013.
- [16] S. Markov, L. Gerrer, F. Adamu-Lema, S. Amoroso, and A. Asenov, “Time domain simulation of statistical variability and oxide degradation including trapping/detrapping dynamics,” in *Proc. Int. Conf. Simul. Semicond. Process. Devices*, 2012, pp. 157–160.
- [17] S. Amoroso, L. Gerrer, S. Markov, F. Adamu-Lema, and A. Asenov, “Comprehensive statistical comparison of RTN and BTI in deeply scaled MOSFETs by means of 3D ‘atomistic’ simulation,” in *Proc. Eur. Solid-State Device Res. Conf.*, Sep. 2012, pp. 109–112.
- [18] M. Krčmar, W. Saslow, and M. Weimer, “Electrostatic screening near semi-conductor surfaces,” *Phys. Rev. B*, vol. 61, no. 20, pp. 13821–13832, 2000.